IJESRT

INTERNATIONAL JOURNAL OF ENGINEERING SCIENCES & RESEARCH TECHNOLOGY

Design and Perform the Optimization of Induction Motors during Voltage-Controlled Soft Starting

S.Sathish Kumar[*1] ,Dr.R.Meenakumari[2],P.Ravikumar[3], A.Anix Salomon[4]

[*1, 2, 3, 4] Jansons Institute of Technlology,Coimbatore, Kongu Engineering College, India

sat_meae2k5@rediffmail.com

Abstract—

This research paper deals with ideas of the design and performance optimization of medium/high-power induction motors during soft starting by eliminating the supply frequency torque pulsations, and by keeping the line current constant at the preset value. Starting torque pulsa- tions are eliminated by triggering back-to-back-connected thyris- tors at proper points on the first supply voltage cycle. Line cur- rent during starting can be kept constant at any preset value by a simple strategy composed of successive sinusoidal and constant function segments of the triggering angle. These strategies are im- plemented by the use of an 8-b microcontroller. Transient perfor- mance analyses of the system are carried out by means of a hybrid ABC/dq machine model which takes into account the three-phase, two-phase, and disconnected modes of operation in terms of actual stator variables. Experimental results obtained on a custom-design test bed are found to be in approximate agreement with the theoretical ones.

Keywords: Induction motor, soft starter, torque pulsations.

I. INTRODUCTION

DIRECT-ONLINE starting of large ac motors may present difficulties for the motor itself, and the loads supplied from the common coupling point because of the voltage dips in the supply during starting, especially in the case of a weak power system [1]–[4]. An uncontrolled starting may cause a trip in either the overload or the undervoltage relay, resulting in starting failure. This is troublesome for field engineers since the motor cannot be reenergized until it cools down to an allowable temperature, in a long time period. Furthermore, the number of starts per day is limited to only a few attempts. Therefore, current and torque profiles of the motor during starting are to be carefully tailored according to the needs of the load.

AC motor starters employing power semiconductors are being increasingly used to replace electromagnetic line starters, and conventional reduced voltage starters because of their controlled soft-starting capability with limited starting current. These may be classified in two groups:

i) back-to-back connected thyristor-based soft starters, which apply a reduced voltage to the motor;

ii) insulated gate bipolar transistor (IGBT) or gate turn-off thyristor (GTO)-based dc link converters, which give a variable-frequency output.

At the present time, pre-engineered versions of such ac motor starters are commercially available up to an operating voltage level of 15 kV l-l, and a power rating of 20 000 hp. With the present technology, the higher cost, complexity, and larger volume occupied by the variable-frequency dc link converter can be largely offset both by the high starting torque requirement of “heavy to start” industrial loads, and the need for speed control in a moderate range. Speed control in a wider range makes necessary special or additional means of cooling for the motor. Thyristorized soft starters, however, are cheap, simple, reliable, and occupy less volume, and hence, their use is a viable solution to the starting problem of medium-voltage and large ac motors, in applications where the starting torque requirement of the load is not high.

Besides the developments and progress in commercial soft starter technology numerous attempts have been made on the performance analyses and control techniques of three- phase induction motors fed from a thyristorized voltage-con- troller .

An induction motor (IM) may produce severe pulsations in electromechanical torque depending upon the initial switching instants of all three-phases to the supply, regardless of the starting method: direct-online or soft starting. Minimiza- tion of the pulsating torque component is given for direct-online starting. The amount of electromagnetic torque pulsations reflected to the shaft depends on the parameters of the mechanical subsystem . These may cause shocks to the driven equipment, and damages in the mechanical system components, such as couplings and gears, in the long term.

In this paper, the performance of the IM during voltage-controlled soft starting has been optimized by eliminating the supply frequency torque pulsations, and by keeping the line current constant at the preset value, over the entire soft-starting period. The pulsating torque elimination strategy defined, and applied in for direct-online starting of the IM has been extended to cover all of the operating conditions of a soft starter, with back-to-back-connected thyristors on each of

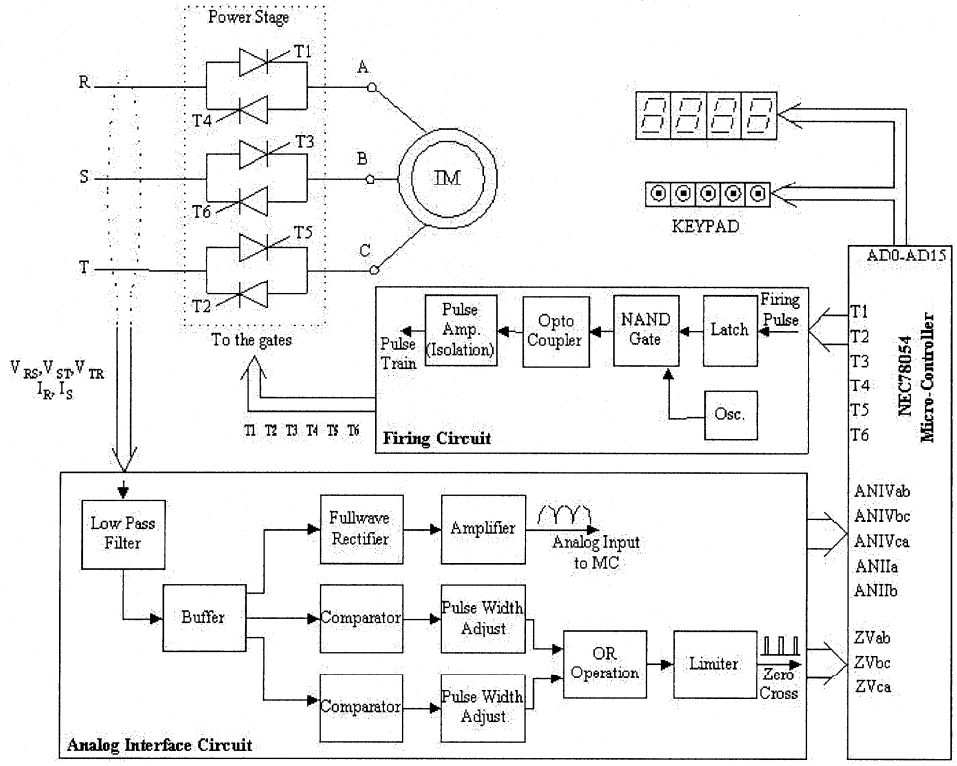

Fig. 1. Block diagram of the soft starter.

the supply lines connected to the stator terminals. The torque pulsation elimination strategy defines the initial triggering instants of the soft starter thyristors on the first supply voltage cycle, for different operating conditions of the soft starter. Furthermore, a current control strategy composed of successive cosinusoidal, and constant function segments of the triggering angle, has been proposed to keep the line current within a desired band at startup, so as to obtain better acceleration profiles during soft-starting, as compared to well-known techniques. The combined performance of the proposed current control, and torque pulsation elimination strategies has been assessed in comparison with other well-known soft starting methods employed. Transient performance analyses of the resulting soft starter have been carried out by means of a hybrid ABC/dq model, which takes into account the three-phase, two-phase, and disconnected modes of operation in terms of the actual stator variables. Theoretical results have been verified experimentally on a custom-design test-bed composed of a laboratory machine set, and a shaft torque measuring system in the dynamic state.

II. System Description and Operation Principles

A detailed block diagram of the soft starter is given in Fig. 1. It is composed of three pairs of back-to-back connected thyristors, a microcontroller (μC)-based control and protection circuitry, pulse shaping and firing circuits, and the analog interface circuit. The analog interface circuit receives the three line-to-line voltage, and two line current signals via potential transformers, and Hall effect current transducers, respectively. Only one of these current signals is used as the feedback signal in order to keep the current constant at the preset value during starting period. Current in the third line can be deduced from the two signals by the μC. These will then be used for protection purposes against overload, unbalanced operation, and faults. The three line-to-line voltage signals are used only for zero-voltage detection, and protection against under and overvoltages. During soft starting, either the true root mean square (rms) values or the peak values of the line currents can be kept constant at a preset value. In the implementation, peak value of the fundamental component has been used in the closed-loop control circuit via the fourth-order Butterworth filter. The two line current waveforms are fully rectified after being filtered, as in the case of voltage signals, for protection purposes. User-interface part of the system consists of status light-emitting diodes (LEDs), alarm LEDs, selection indicator LEDs, keypad, and seven segment displays. Keypad is used to input set value of the line current and the rated current, and to recreate the acceleration profile.

For RST phase sequence of the supply voltages, thyristors of the voltage controller are to be triggered in a sequence as marked on Fig. 1, resulting in a phase difference of 60° between consecutive switchings during starting as well as in the steady state, excluding the first energization cycle. In order to eliminate the electromagnetic (EM) torque pulsations at the supply frequency, different switching strategies have been used for T1, T2, and T3, on the first supply voltage cycle for continuous, and discontinuous line current cases, depending on whether the triggering angle "α" is less or greater than the pf angle of the machine at unity slip. In order to ensure constant current during

starting, a simple control strategy composed of successive cosinusoidal and constant function segments of "α" is employed, as described in Section IV. The soft starter developed in this work has some further features such as estimating initial firing angle value for the current setting, storing successful load and current setting-dependent run-ups, etc. In the starting period, at any point on the acceleration profile, the IM will operate in one of the following three operation states depending upon the power factor of the motor, and starting current limit setting: 1) three-phase operation; 2) two-phase operation; and 3) no-phase operation (disconnected mode).

The analysis and design work of the system are carried out by using hybrid models, in which the stator quantities are kept in their actual form, whereas rotor quantities are transferred into a reference frame fixed in the stator.

III. Mathematical Model of System

The mathematical models used in the digital simulation of the system are given in this section. The numerical solution method, and necessary transitions between various operation modes of the starter are described. At any time, the IM operates in one of the operation modes defined in Table I.

A. Three-Phase Model

Starting with the mathematical model of the IM in terms of ABC/abc axes quantities, all space angle, and hence, time variations in inductances are eliminated by applying the well- known three-phase to two-phase, and commutator transformations ($\mathbf{C_1}$ and $\mathbf{C_2}$), only to the rotor side. This results in a hybrid mathematical model in terms of ABC/dq0 axes quantities for which the rotor reference frame is fixed in the stator [21]. The hybrid model is brought into the state space form for digital simulation, as given in (1), shown at the bottomo of the page, and (3), shown on the next page.

B. Two-Phase Models

1) Mode 1: When only motor terminals A and B are connected to the supply, the two-phase model in (4) and (5), shown on the next page, is to be used. Since $i_C = 0$ and $i_B = -i_A$, the behavior of the motor is expressed in terms of the line-to-line voltage V_{AB}.

TABLE I
Definition of Operation Modes

Operation mode	*Operation type*	*Motor terminals connected to supply*
Mode 0	3-phase	ABC
Mode 1	2-phase	AB
Mode 2	2-phase	AC
Mode 3	2-phase	BC
Mode 4	No-phase	none

2) Mode 2: This operation mode arises when motor terminals A and C are connected to the supply. By substituting $i_B = 0$ and $i_C = -i_A$into the mathematical model, and making the necessary row operations, (6) and (7), shown on the next page, are obtained.

3) Mode 3: This operation mode arises when motor terminals B and C are connected to the supply. By substituting $i_A = 0$ and $i_C = -i_B$, the mathematical model in (8) and (9), shown on the next page, is obtained.

C. No-Phase Operation (Disconnected Mode)

The mathematical model in (10) is used for the case where none of the motor terminals is connected to the supply. Since $i_A = i_B = i_C = 0$, only the rotor voltage equations are to be solved in the transient-state

$$p\begin{bmatrix} i'_q \\ i'_d \end{bmatrix} = \begin{bmatrix} -R'_2/L'_2 & w_r \\ -w_r & -R'_2/L'_2 \end{bmatrix} \begin{bmatrix} i'_q \\ i'_d \end{bmatrix} \qquad Te = 0. \tag{10}$$

D. Numerical Solution Method

To solve for the nonlinear first-order differential equation sets given above, a fourth-order Runge–Kutta integration algorithm is used. To ensure the continuity of solutions when a change in the operation mode takes place, final values of the previous mode are taken as initial values of the next mode. This first necessitates the detection of turn-off instant for the conducting thyristor in one of the three supply lines. This is achieved by the "Current Zero Detection Subroutine" integrated

$$p\begin{bmatrix} i_A \\ i_B \\ i'_q \\ i'_d \end{bmatrix} = \begin{bmatrix} -2BR_1 & -(2\sqrt{6}/3)AM'w_r & (2\sqrt{6}/3)BM'w_r & -(2\sqrt{3}/3)AR'_2 \\ -(\sqrt{6}/3)AM'w_r & -2BR_1 & -AR'_2 - (\sqrt{6}/3)BM'w_r & (\sqrt{3}/3)AR'_2 \\ (2\sqrt{6}/3)AM'w_r & +(\sqrt{6}/3)AM'w_r & & -\sqrt{2}BM'w_r \\ (\sqrt{6}/2)M'w_r(A^2/B + 1/L'_2) & -2AR_1 & -A^2R'_2/B - R'_2/L'_2 & w_r - \sqrt{2}AM'w_r \\ -AR_1 & & & \\ (1/2)Aw_rB - \sqrt{3}AR_1 & Aw_rB - \sqrt{2}A^2M'w_r/B & -w_r + \sqrt{2}AM'w_r & -A^2R'_2/B - R'_2/L'_2 \\ -(\sqrt{2}/2)A^2M'w_r/B & & & \end{bmatrix} \cdot \begin{bmatrix} i_A \\ i_B \\ i'_q \\ i'_d \end{bmatrix} + \begin{bmatrix} (2/3)B & (2/3)B \\ -(4/3)B & (2/3)B \\ -A & A \\ (\sqrt{3}/3)A & \sqrt{3}/3A \end{bmatrix} \cdot \begin{bmatrix} V_{AB} \\ V_{AC} \end{bmatrix} \tag{1}$$

into the program. Forward or backward thyristor in one of the supply lines turns off when its current ceases. "Current Zero Detection Subroutine" monitors continuously the current, and whenever it takes a negative value at any numerical integration step "m," the program terminates and returns to the previous integration step "$m-1$," to detect the zero crossing point with an acceptable error, at a reduced time step. The next operation mode can then be determined automatically by detecting the forward biased thyristors, which receive a firing pulse.

Possible transitions from old to new operation modes are given column wise in Tables II–VI. If the current of forward or backward thyristor in any one of the three lines ceases before the antiparallel thyristor receives a firing pulse, possible operation mode is either the two-phase or the no-phase operation. If a thyristor in one of the lines receives a firing pulse while the others are not conducting, it cannot trigger into conduction until a reverse thyristor in one of the other two lines receives a firing pulse, resulting in no-phase operation. In Table II, transitions from three-phase to two-phase operation are given. This occurs if "α" is greater than the power factor angle "θ" of the motor. However, in cases where $\alpha \leq \theta$, both the new and old operation modes are three-phase operation. "θ" value depends on the operating condition, especially on the shaft speed, and can be determined from the per-phase equivalent circuit at the steady state. Transitions from two-phase operation modes (1 to 3) to any other are given in Tables III–V. In Tables II–VI, thyristors marked as active for no-phase operation are not in conduction state, but they are only receiving firing pulses.

TABLE II
TRANSITIONS FROM MODE 0 TO OTHERS

Active thyristors	123	234	345	456	561	612
Old Mode	0	0	0	0	0	0
Active thyristors	23	34	45	56	61	12
Motor terminals connected to supply	BC	AB	AC	BC	AB	AC
New Mode	3	1	2	3	1	2

TABLE III
TRANSITIONS FROM MODE 1 TO OTHERS

Active thyristors	61	34	61	34	61	34
Old Mode	1	1	1	1	1	1
Active thyristors	612	345	12	45	1	4
Motor terminals connected to supply	BAC	BAC	AC	AC	none	none
New Mode	0	0	2	2	4	4

Where

$$A = \sqrt{2}BM'/L_2', \quad \text{and} \quad B = 1/(2L_1 - 2M'^2/L_2')$$

$$T_e = -(pp)((\sqrt{6}/2)M'i_q'i_A + (\sqrt{2}/2)M'i_d'i_A + \sqrt{2}M'i_d'i_B) \tag{2}$$

$$pw_r = (1/J)(T_e - T_L) \tag{3}$$

$$p\begin{bmatrix} i_A \\ i_q' \\ i_d' \end{bmatrix} = \begin{bmatrix} -2R_1B & (\sqrt{6}/2)M'w_rB + (1/2)AR_2' & (\sqrt{2}/2)M'w_rB - (\sqrt{3}/2)AR_2' \\ -(\sqrt{3}/2)Aw_r/B + AR_1 & -(\sqrt{6}/4)AM'w_r - R_2'/L_2' + (1/4)A^2R_2'/B & (\sqrt{3}/4)A^2R_2'/B - (\sqrt{2}/4)AM'w_r + w_r \\ -(1/2)Aw_r/B - \sqrt{3}AR_1 & (3\sqrt{2}/4)AM'w_r + (\sqrt{3}/4)A^2R_2'/B - w_r & (\sqrt{6}/4)AM'w_r - R_2'/L_2' - (3/4)A^2R_2'/B \end{bmatrix} \times \begin{bmatrix} i_A \\ i_q' \\ i_d' \end{bmatrix} + \begin{bmatrix} B \\ -(1/2)A \\ (\sqrt{3}/2)A \end{bmatrix} [V_{AB}] \tag{4}$$

$$T_e = -(pp)((\sqrt{6}/2)M'i_q'i_A - (\sqrt{2}/2)M'i_d'i_A) \tag{5}$$

$$p\begin{bmatrix} i_A \\ i_q' \\ i_d' \end{bmatrix} = \begin{bmatrix} -2R_1B & (\sqrt{6}/2)M'w_rB + (1/2)AR_2' & (1/2)AL_2'w_r - (\sqrt{3}/2)AR_2' \\ -(\sqrt{3}/2)Aw_r/B - AR_1 & (\sqrt{6}/4)AM'w_r - R_2'/L_2' - (1/4)A^2R_2'/B & -(\sqrt{3}/4)A^2R_2'/B - (\sqrt{2}/4)AM'w_r + w_r \\ (1/2)Aw_r/B - \sqrt{3}AR_1 & (3\sqrt{2}/4)AM'w_r - (\sqrt{3}/4)A^2R_2'/B - w_r & (\sqrt{6}/4)AM'w_r - R_2'/L_2' - (3/4)A^2R_2'/B \end{bmatrix} \times \begin{bmatrix} i_A \\ i_q' \\ i_d' \end{bmatrix} + \begin{bmatrix} B \\ -(1/2)A \\ (\sqrt{3}/2)A \end{bmatrix} [V_{AC}] \tag{6}$$

$$T_e = -(pp)((\sqrt{6}/2)M'i_q'i_A + (\sqrt{2}/2)M'i_d'i_A) \tag{7}$$

$$p\begin{bmatrix} i_B \\ i_q' \\ i_d' \end{bmatrix} = \begin{bmatrix} -2R_1B & -AR_2' & -\sqrt{2}M'w_rB \\ -2R_1A & A^2R_2'/B - R_2'/L_2' & -\sqrt{2}AM'w_r + w_r \\ Aw_r/B & -w_r & -R_2'/L_2' \end{bmatrix} \begin{bmatrix} i_B \\ i_q' \\ i_d' \end{bmatrix} + \begin{bmatrix} B \\ 0 \\ A \end{bmatrix} [V_{BC}] \tag{8}$$

$$T_e = -(pp)\sqrt{2}M'i_d'i_B. \tag{9}$$

TABLE IV
TRANSITIONS FROM MODE 2 TO OTHERS

Active thyristors	12	45	12	45	12	45
Old Mode	2	2	2	2	2	2
Active thyristors	123	456	23	56	2	5
Motor terminals connected to the supply	ACB	ACB	CB	CB	none	none
New Mode	0	0	3	3	4	4

TABLE V
TRANSITIONS FROM MODE 3 TO OTHERS

Active thyristors	23	56	23	56	23	56
Old Mode	3	3	3	3	3	3
Active thyristors	234	561	34	61	3	6
Motor terminals connected to the supply	CBA	CBA	BA	BA	none	none
New Mode	0	0	2	2	4	4

TABLE VI
TRANSITIONS FROM MODE 4 TO OTHERS

Active thyristors	1	2	3	4	5	6
Old Mode	4	4	4	4	4	4
Active thyristors	12	23	34	45	56	61
Motor terminals connected to supply	AC	CB	BA	AC	CB	BA
New Mode	2	3	1	2	3	1

IV. RESULTS

The firing angle control strategy, which yields a nearly perfect starting current envelope, and the initial thyristor triggering strategy, which nearly eliminates the torque pulsations, will be described in this section. These strategies are deduced from the results of digital simulation studies, and are verified by experimental work. The proposed strategies are applicable with minor modifications, both to the medium voltage squirrel-cage IM, and to the low-voltage ones.

A. Elimination of Torque Pulsations

The cause of pulsations in electromechanical torque at the supply frequency is the uncontrolled switching of three motor phases to the supply on the first voltage cycle. Simultaneous switching of the three motor phases always gives rise to a considerable pulsating torque component [16]. In solid-state starters for medium-voltage IMs, the switching strategy reported in [21] nearly eliminates the torque pulsations. In direct-online starters, "α" is zero; therefore, the mentioned switching strategy constitutes a special case of the torque pulsation elimination strategy applicable to solid-state soft-starters. In Table VII, the initial switching strategies that can be used in solid-state soft starters

TABLE VII
TRIGGERING INSTANTS OF THYRISTORS ON THE FIRST CYCLE FOR ELIMINATION OF TORQUE PULSATIONS

Thyristor no.	Triggering angle, degrees		
	Continuous line current	Discontinuous Line current	
	Case 1: $\alpha_0 \le \sigma$	*Case 2:* $\sigma < \alpha_0 < \theta_0$	*Case 3:* $\theta_0 \le \alpha_0$
T1	α_0	α_0	α_0
T2	120	$\beta_2(\alpha_0)$	$\alpha_0 + 60$
T3	$120 + 90$	$\beta_2(\alpha_0)+90$	$\alpha_0 + 60+\beta_3(\alpha_0)$
T4	$180 + \alpha_0$	$180 + \alpha_0$	$180 + \alpha_0$
T5	$240 + \alpha_0$	$240 + \alpha_0$	$240 + \alpha_0$
T6	$300 + \alpha_0$	$300 + \alpha_0$	$300 + \alpha_0$

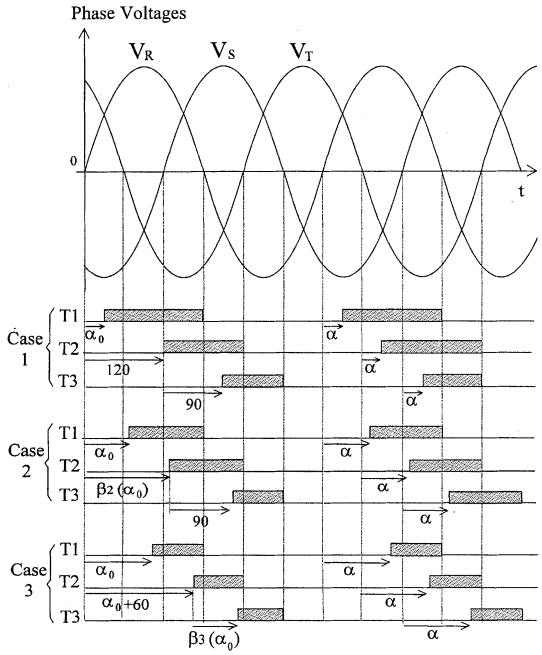

Fig. 2. Torque pulsation elimination strategy.

are given for both the continuous, and discontinuous line current cases. To eliminate the torque pulsations, the six thyristors in Fig. 1 should receive firing pulses in turn (in the numbered sequence from 1 to 6), at prespecified points of the first supply voltage cycle, as illustrated in Fig. 2. Continuity of the line current waveform is largely dictated by the initial setting of firing angle "α_0," which adjusts the starting current to the preset value. For the discontinuous line current case, two different initial switching strategies would arise, depending upon whether "α" is less or greater than the power factor angle of the IM at unity slip "θ_0." For most standard NEMA Class A, and B squirrel-cage IM under 1000 hp, typical data suggest the assumption of starting pf as being nearly equal to 0.2 [1].

The transition between continuous and discontinuous line current waveforms occurs for an α range smaller than, but close to the pf angle at unity slip (i.e., $\sigma < \alpha_0 < \theta_0$). At the critical angle "σ," some of the line currents become discontinuous in the first cycle, and during a considerable portion of the acceleration period, all line currents become continuous. Similar to

the starting pf, only minor changes occur in "σ" for class A and B squirrel-cage IM. Indeed, "σ" is found to be 63° and 65°, respectively, for the low-voltage and medium-voltage IMs.

In Table VII, firing angles of all thyristors are defined with respect to the zero-crossing point on the ascending portion of phase R voltage. First, T1 receives a firing pulse at "α_0," but it does not trigger into conduction until T2 receives a firing pulse at 120° for case 1, "$\beta_2(\alpha_0)$" for case 2, and "$\alpha_0 + 60°$" for case 3. This initiates the two-phase operation. The next thyristor which is going to be triggered into conduction is T3, which receives its firing pulse with a delay of 90° for cases 1 and 2, and "$\beta_3(\alpha_0)$" for case 3. In the elimination of torque pulsations, only these two switching instants for T2 and T3 are important; the remaining thyristors T4 to T6 will receive firing pulses in the normal sequence with delays of 180°, 240°, and 300° with respect to "α_0." Expressions of "$\beta_2(\alpha_0)$" and "$\beta_3(\alpha_0)$" are given in (11) and (12), respectively. The coefficients of these straight lines have been found within ± 1 % accuracy from the results of simulation studies, by curve fitting techniques. For this purpose, several trials have been made in order to eliminate the torque pulsations for different initial firing angle settings. Major changes in the coefficients of straight lines have not been observed from low-voltage IMs to medium voltage ones. Therefore, a common set of straight line equations for the optimum triggering instants of T2 and T3 can be used. These would nearly eliminate, or minimize the pulsating torque component for machines of different sizes. Initial α values, which are considerably smaller than the pf angle at unity slip, yield continuous line current waveforms (case 1 in Table VII). For a loaded motor, as the speed increases during starting, motor pf increases too. However, this will not be the case if the motor is going to be accelerated at no load or light load. It is obvious that a firing angle control range from zero to the critical firing angle "σ" at unity slip (case 1) results in no soft starting action over a considerable portion of the starting

$$\beta_2(\alpha_0) = 1.75\alpha_0 + 5.50 \quad (11)$$

$$\beta_3(\alpha_0) = -0.63\alpha_0 + 143.70 \quad (12)$$

period. The three line currents remain continuous, and the soft starter behaves just like a direct-online starter during acceleration. However, as the speed increases, θ gradually decreases, and may have a value lower than α setting in the steady state. Therefore, this operating condition gives rise to discontinuous line current waveforms, and hence, to pulsations in the electromagnetic torque at six times the supply frequency in the steady state. For case 2, some of the line current waveforms become discontinuous (during current holdoff angle γ), and during a considerable portion of the starting period, all current waveforms become continuous. A sample waveform set is given in Fig. 3. When $\alpha_0 > \theta_0$, the line currents become discontinuous over the entire starting period (case 3 in Table VII). A sample waveform set is given in Fig. 4. It has been shown in [16] that the transient supply frequency torque component at starting of the IM is almost entirely dependent on the transient asymmetrical magnetizing current. In view of the very high value of $\omega L/R$, with respect to the magnetizing current, it is necessary to connect each phase to the corresponding supply voltage at or near

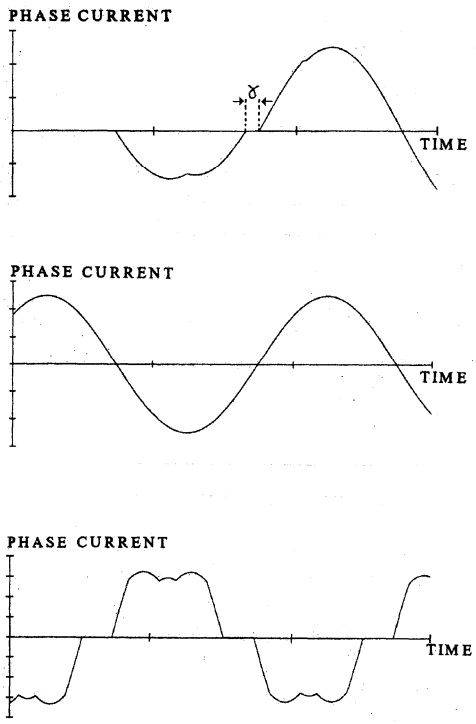

Fig. 3. Line current waveforms for case 2 at = 75° [Time scale: 10 ms/div; (top), (middle) phase current during starting (100 A/div); (bottom) phase current at steady state (20 A/div)].

the instant of maximum value, to minimize this transient component. Starting from the expression of per unit magnitude of supply frequency torque component given in [16] for direct-online starting, the per unit value of the supply frequency torque component produced by an IM during soft-starting can be expressed approximately as given in (13)

$$T_{50\ Hz} \approx [\cos^2(\beta_2(\alpha_0) - \pi/6 - \gamma/2) + \sin^2(\beta_2(\alpha_0) - \pi/6 - \gamma/2 + \beta_3(\alpha_0))]^{1/2} \quad (13)$$

where γ is the stator current holdoff angle in the first cycle, as indicated on Fig. 3. "γ" depends on α_0, and remains almost the same for all IMs with a starting pf in the range 0.2–0.3. Note that $T_{50\ Hz}$ is minimized when both $\beta_2(\alpha_0) - \pi/6 - \gamma/2 = 90°$ and $\beta_2(\alpha_0) - \pi/6 - \gamma/2 + \beta_3(\alpha_0) = 180°$. Here, since $\beta_2(\alpha_0)$ is expressed with respect to the zero-crossing of phase R voltage, a phase-shift of $\pi/6$ rad. occurs with respect to V_{RT}. For relatively high values of initial firing angles (i.e., $\alpha_0 > 100°$), a significant sixth-order torque ripple superimposes on the supply frequency oscillations. This brings a further delay to the optimum initial switching instants, which can only be determined by means of numerical simulations.

For the elimination of supply-frequency torque pulsations, the soft starter selects one of the control strategies which are defined as Case 1 to 3 in Table VII, by comparing "α_0" with the boundaries "σ," and "θ_0," (i.e., case 1: $\alpha_0 \leq \sigma$, case 2: $\sigma < \alpha_0 < \theta_0$, case 3: $\theta_0 \leq \alpha_0$). Since minor changes occur in the values of "σ" and "θ_0" from one motor to another, torque pulsations will be nearly eliminated by using fixed values such as $\sigma = 65°$ and $\theta_0 = 75°$. Motor-dependent adjustment of "σ"

ISSN: 2277-9655

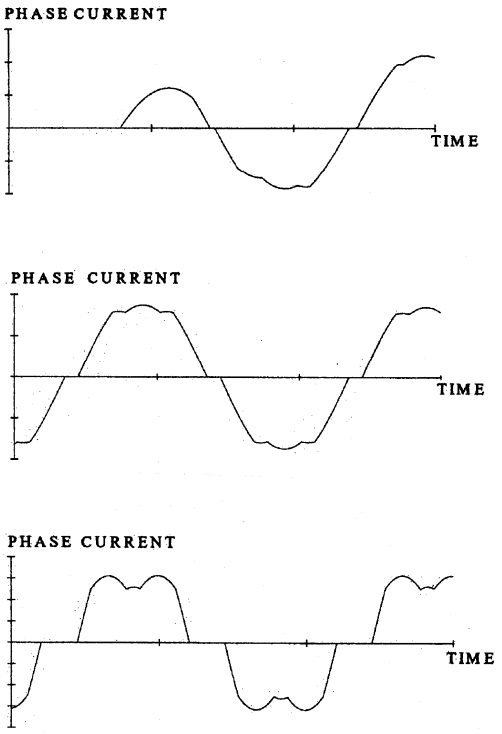

Fig. 4. Line current waveforms for case 3 at = 83 . [Time scale: 10 ms/div; (top), (middle) phase current during starting (100 A/div); (bottom) phase current at steady state (20 A/div)].

and "θ_0" (e.g., $\sigma = 63°$ and $\theta_0 = 73°$), however, eliminates entirely the torque pulsations. There remains the determination of α_0 by the μC for the given motor, and the set value of current limit. This can be achieved by using one of the methods given below in the order of complexity:

1) starting with a sufficiently large α_0 value (e.g., $\alpha_0 = 120°$) and using closed-loop current control strategy;
2) motor-dependent lookup table;
3) calculating from the per-phase equivalent circuit by the use of motor parameters;
4) parameter estimation based on one cycle energization of the motor.

B. Current Control Strategy

A simple current control strategy is proposed to keep the starting current constant at the preset value. This closed-loop current control strategy is implemented by the use of a μ C, and gives nearly level envelopes for the starting current waveforms. As illustrated in Fig. 5, the proposed current control strategy is composed of successive cosinusoidal and constant function segments of "α" in accordance with the feedback signal taken from one of the line currents. Starting current limit can be set to any value in the range from $I_{n(peak)}$ to $kI_{n(peak)}$ by the operator, where $I_{n(peak)}$ and k are the peak value of rated motor current, and the index indicating the limit value of starting current, respectively. k varies in the range from 1 to 5–8, depending on the motor. The controller acts with respect to a limit value which is chosen to be only a few percentages smaller than $kI_{n(peak)}$. Here, the purpose is to keep fluctuations in the current around

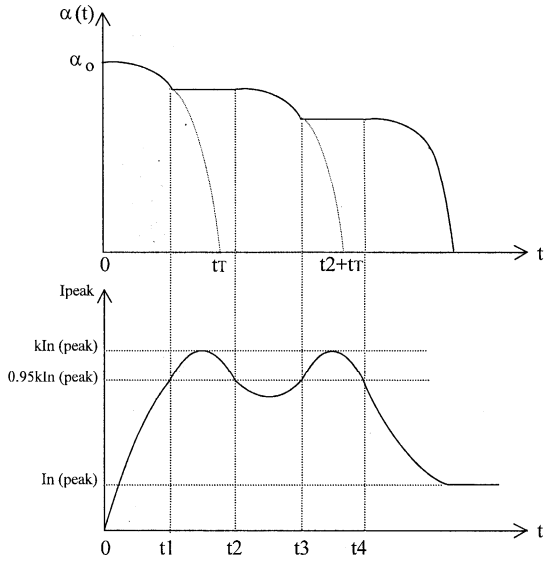

Fig. 5. Illustration of proposed starting current limiting strategy.

$kI_{n(peak)}$. In Fig. 5, this lower limit value at which the controller acts has been chosen as $0.95kI_{n(peak)}$.

In Fig. 5, α_0 is the initial firing angle estimated by the controller, and gives the preset value of starting current just at the switching instants. t_T is the period of the quarter of cosinusoidal α variation, and 0.95 is the lower limit of the band defined for the starting current. t_T, and the lower band limit constant determine the success of the starting current pattern. Choosing t_T value unnecessarily large will cause an extended starting time duration; however, the starting current pattern will be perfectly smooth. Choosing t_T too small will result in an increased number of cosine and constant "α" segments, during start-up. This would cause a distorted and undesirable starting current pattern tending to move outside the chosen band. t_T, and the lower band limit constant can be reprogrammed optimally by the application engineer using the field experience, and depending upon the size of the motor and load characteristics, if necessary. By means of sensitive programming, the possibility of high inrush currents is eliminated, and the starting current waveform approximates more closely to a waveform with ideal envelopes. After energizing the motor at $t = 0$, "α" is varied by the controller cosinusoidally until the current reaches, and then tends to exceed the lower limit of the band: $(0.95kI_{n(peak)})$ at $t = t1$. The current controller then keeps "α" constant at $\alpha(t1)$ until the current returns to $0.95kI_{n(peak)}$ after making an overshoot.

At time t2, the controller replaces constant "α" by cosinusoidal variation, resulting in an undershoot in starting current envelope in the time period from t2 to t3. The controller action repeats itself in this manner until the motor reaches the full speed. It is worth noting that the variations in Fig. 5 are not drawn to scale, and are exaggerated in order to illustrate the operation principles of the current controller. At the final speed, "α" reaches zero.

Line current and EM torque waveforms during starting of the same medium-voltage IM are given in Fig. 6 for a current limit value of $3.3I_n$.

Following observations can be made on these waveforms:

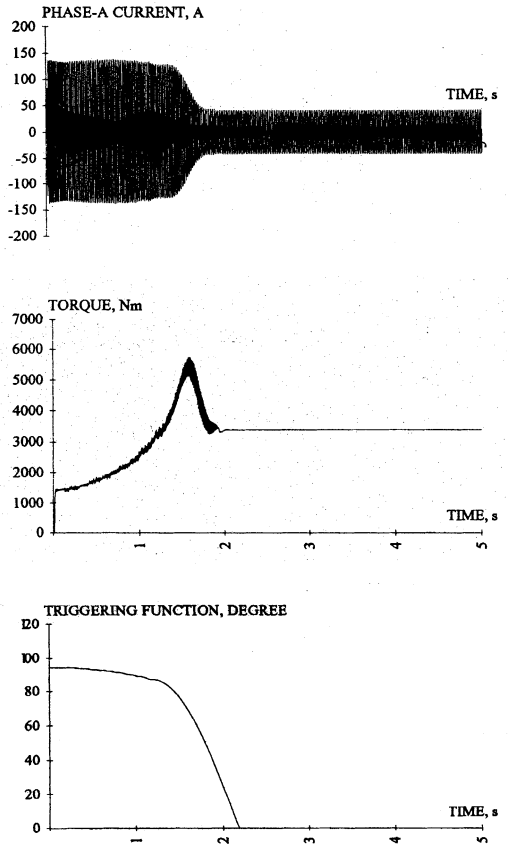

Fig. 6. Line current and electromagnetic torque versus time for $I = 3.3I_n$.

1) starting current remains nearly constant at the preset value;
2) starting torque pulsations at the supply frequency are successfully eliminated;
3) since the line currents are discontinuous during starting, torque pulsations at six times the supply frequency with relatively low amplitudes, are produced;
4) Since too many transitions would occur between cosine and constant function segments, and the control band $kI_{n(peak)} - 0.95kI_{n(peak)}$ is narrow, $\alpha(t)$ versus t and I_{peak} versus t variations are not as marked as in Fig. 5.

C. Experimental Results

The performance of the developed soft starter equipped with torque pulsation elimination, and starting current control strategies is tested on a 4-kVA, 0.4-kV laboratory motor-generator set equipped with a custom-design torque and speed measuring system in the dynamic state.

Fig. 7 shows the variations in the shaft torque and starting current of the soft starter for $3I_n$ current setting. As can be understood from Fig. 7(top), simultaneous connection of the three motor terminals to the supply causes severe pulsations in the shaft torque. If the thyristors of the soft starter were triggered at "α_0," "$\alpha_0 + 60°$," "$\alpha_0 + 120°, \ldots,$ on the first applied voltage cycle, the response of the system would be as in Fig. 7(middle). This switching strategy yields less pulsations in the shaft torque in comparison with simultaneous switching. The proposed switching strategy, however, eliminates entirely

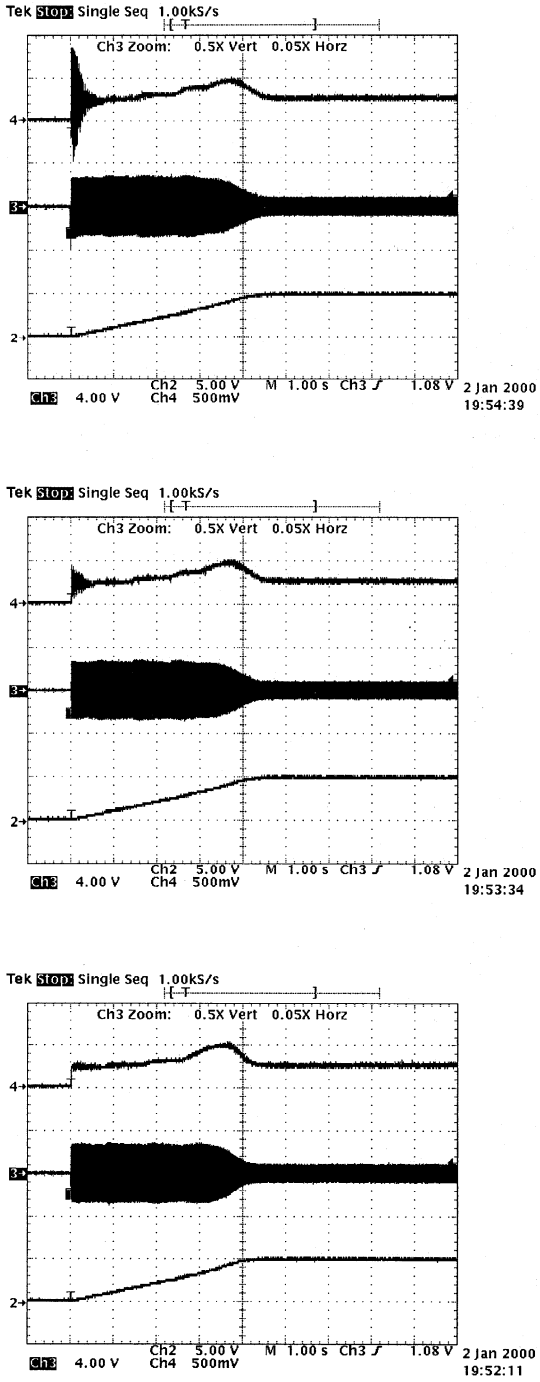

Fig. 7. Starting performances of the system with the proposed current control method (Ch4: Shaft torque, 50 Nm/div; Ch3: Line current, 60 A/div; Ch2: Speed, 1500 r/min/div). (top) Simultaneous switching, (middle) all phases switched at = 72º , (bottom) proposed pulsating torque elimination strategy.

the shaft torque pulsations, and reduces the starting time of the motor-load combination, as shown in Fig. 7(bottom).

A set of starting current versus time waveforms is presented in Fig. 8 for a comparative assessment of the known open-loop triggering strategies (ramp and cosinusoidal triggering functions), and the proposed closed-loop current limiting strategy. In these case studies, the pulsating torque elimination strategy has been applied, and the output of the driven machine has been

ISSN: 2277-9655

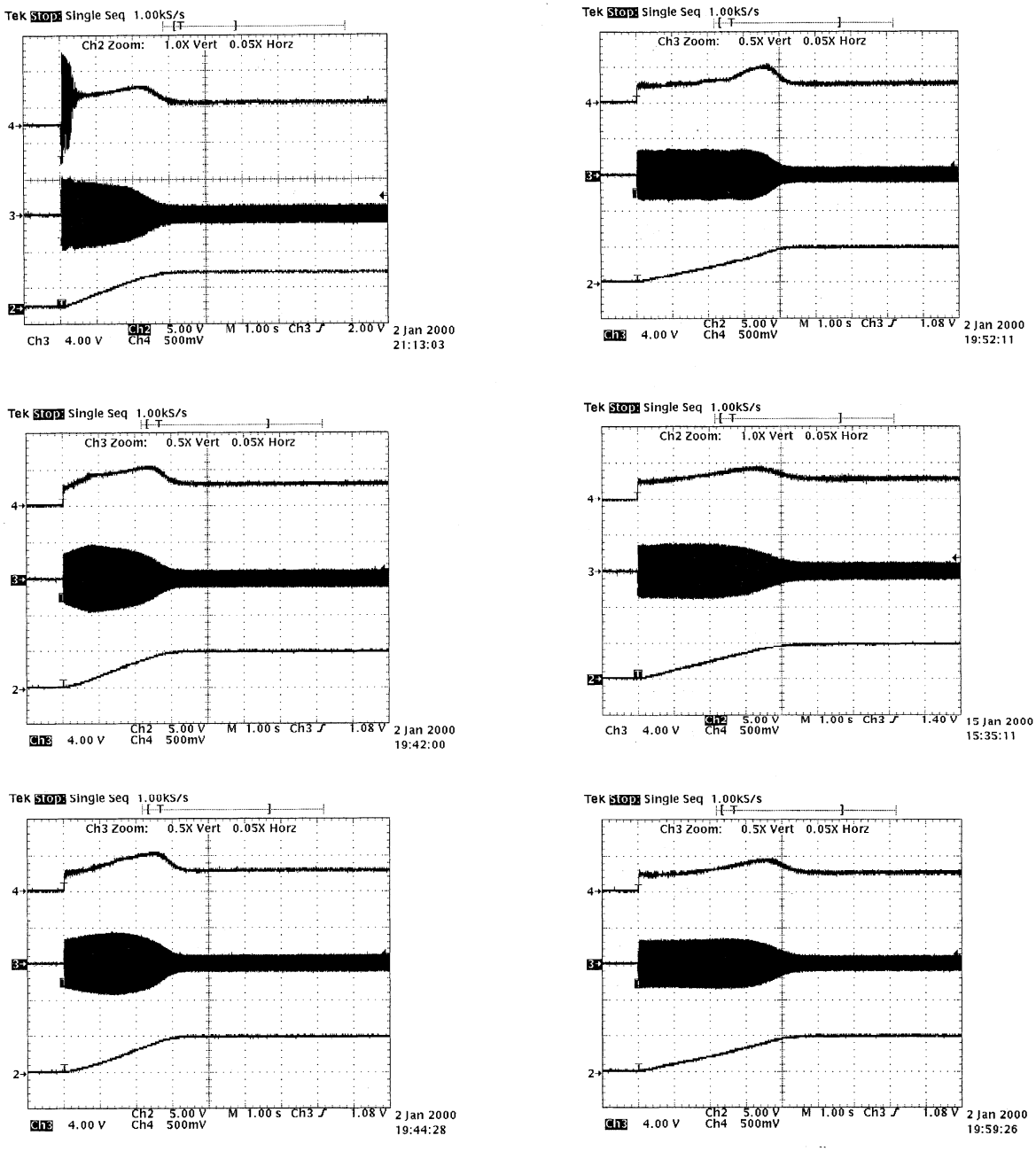

Fig. 8. Comparison of starting performances of various current control strategies with pulsating torque elimination. (top left) Direct-online starting without torque elimination. (middle left) Ramp triggering function. (bottom left) Cosine triggering function. (top right) Cosine-constant triggering function. (middle right) Ramp triggering with ramp time $T = 15$ s. (bottom right) Cosine triggering with period $T = 7$ s.

adjusted to the nominal value at steady-state. Direct-online starting in Fig. 8(top left) is given only for comparison purposes. In Fig. 8(middle left) and (bottom left), the firing angle of soft-starter thyristors is varied, respectively, as ramp and cosine functions during starting. The following observations are made on these waveforms.

- The starting current does not remain constant, and especially for ramp triggering function, may follow the direct-online starting current envelope as the motor speed increases.
- The periods of ramp and cosinusoidal triggering functions in which "α" is varied from "α_0" to zero, are dependent on the motor and load characteristics. For the load considered in Fig. 8, longer time periods would approximate the starting current more closely to a constant current waveform.

However, for the current control strategy proposed in this work, the starting current can be successfully kept constant at a preset value, with nearly level envelopes, during the starting period [Fig. 8(iv)]. Since the control exercised on the starting current is closed-loop control, the proposed control system inherently takes into account load characteristics. Note that the periods of ramp [Fig. 8(ii)], and cosinusoidal [Fig. 8(iii)] "α" variations are adjusted to the starting period of cosine-constant triggering function [Fig. 8(iv)] which is 4.2 s.

In order to approximate the starting current envelopes to ideal ones for the ramp and cosinusoidal triggering functions, several trials have been made. The optimum cases are as given in Figs. 8(v) and (vi). Corresponding variation periods are 15 and 7 s, which are longer than the "α" variation period of the proposed current control strategy. A good correlation is obtained between the theoretical and experimental results.

V. Conclusion

Performance optimization of a voltage-controlled, thyristorized induction motor soft starter is carried out by the use of some simple control strategies implementable on a microcontroller at no additional cost. Nearly perfect current and torque profiles can be obtained during starting for better utilization of the available starting facilities. Using the proposed strategies, a good acceleration profile can be tailored by smooth, pulsation-free torques over the entire starting period. Since soft starting by voltage control reduces the starting torque with the square of the ratio of applied rms voltage to rated voltage, the applicability of this method depends on the stiffness of the grid, and torque requirement of the load. On the other hand, for loads with high starting torque requirement, and operating on very weak grids, the only alternatives are starting by frequency control or by conventional techniques employing wound rotor induction motors, for which high torques can be produced at low currents.

References

[1] A. J. Williams and M. S. Griffith, "Evaluating the effects of motor starting on industrial and commercial power systems," *IEEE Trans. Ind. Applicat.*, vol. IA-14, pp. 292–299, July/Aug. 1978.

[2] F. M. Bruce, R. J. Graefe, A. Lutz, and M. D. Panlener, "Reduced-voltage starting of squirrel-cage induction motors," *IEEE Trans. Ind. Applicat.*, vol. IA-20, pp. 46–55, Jan./Feb. 1984.

[3] P. J. Colleran and W. E. Rogers, "Controlled starting of AC induction motors," *IEEE Trans. Ind. Applicat.*, vol. IA-19, pp. 1014–1018, Nov./Dec. 1983.

[4] J. Nevelsteen and H. Aragon, "Starting of large motors-methods and economics," *IEEE Trans. Ind. Applicat.*, vol. 25, pp. 1012–1018, Nov./Dec. 1989.

[5] F. Blaabjerg, J. K. Pedersen, S. Rise, H. H. Hansen, and A. M. Trzynadlowski, "Can soft-starters help save energy," *IEEE Ind. Applicat. Mag.*, vol. 3, pp. 56–66, Sept./Oct. 1997.

[6] J. Bowerfind and S. J. Campbell, "Application of solid-state AC motor starters in the pulp and paper industry," *IEEE Trans. Ind. Applicat.*, vol. IA-22, pp. 109–114, Jan./Feb. 1986.

[7] W. Shepherd, "On the analysis of the three phase induction motor with voltage control by thyristor switching," *IEEE Trans. Ind. General Applicat.*, vol. IGA-4, pp. 304–311, May/June 1968.

[8] S. A. Hamed and B. J. Chalmers, "Analysis of variable-voltage thyristor controlled induction motors," *Proc. Inst. Elect. Eng., B*, vol. 137, no. 3, pp. 184–193, May 1990.

[9] S. S. Murthy and G. J. Berg, "A new approach to dynamic modeling and transient analysis of SCR controlled induction motors," *IEEE Trans. Power App. Syst.*, vol. PAS-101, pp. 219–229, Sept. 1982